Abdelkader Abdallah[1], Abdelkader Chaker [2] Tayeb Allaoui [3]

Laboratory SCAMRE Department of Electrical Engineering, E.N.P Oran (1),
ORAN Polytechnic School (2), L2GEGI LaboratoryUniversity Tiaret (3)
ORCID.

doi:10.15199/48.2021.11.02

An adaptive RST fuzzy logic and an adaptive PI fuzzy logic controllers of a DFIG in Wind Energy Conversion

Abstract. *This paper proposes an adaptive logic controllers for a wind energy conversion system (WECS) based on doubly fed induction generator (DFIG). Active and reactive power flow is controlled simultaneously with a four control methods of the active and reactive currents. These include a direct PI controller, A RST controller, an adaptive fuzzy logic PI (AFLC-PI) and an adaptive RST fuzzy logic with virtual reference (VFLC-RST) controls. The results demonstrate that VFLC-RST are very effective in improving the transient power system stability and very robust against variable transmission line parameters*

Streszczenie. *W artykule zaproponowano adaptacyjne sterowniki logiczne dla systemu konwersji energii wiatru (WECS) opartego na podwójnie zasilanym generatorze indukcyjnym (DFIG). Przepływ mocy czynnej i biernej jest kontrolowany jednocześnie za pomocą czterech metod regulacji prądów czynnych i biernych. Obejmują one bezpośredni kontroler PI, kontroler RST, adaptacyjną logikę rozmytą PI (AFLC-PI) i adaptacyjną logikę rozmytą RST ze sterowaniem wirtualnym odniesieniem (VFLC-RST). Wyniki pokazują, że VFLC-RST są bardzo skuteczne w poprawianiu przejściowej stabilności systemu zasilania i bardzo odporne na zmienne parametry linii przesyłowej. (**Adaptacyjna logika rozmyta RST i adaptacyjne sterowniki logiki rozmytej PI DFIG w konwersji energii wiatrowej**)*
Wię

Keywords: wind energy, doubly fed induction generator, adaptive fuzzy logic RST, robustness.
Słowa kluczowe: energia wiatrowa, podwójnie zasilany generator indukcyjny, adaptacyjna logika rozmyta RST, solidność.

Introduction

The technology of wind turbines is continually advanced. This allowed, for wind power, to become in recent years an alternative to traditional energy sources. This has made possible the latest generation of wind turbines operate at variable speed. This type of operation has increased energy efficiency, lower mechanical loads and improve the quality of the electrical energy produced, compared to fixed speed wind turbines [1-2].

In this context, we are interested in our study the control of a three-bladed wind turbine based on an asynchronous machine with wound rotor DFIG monitored through the rotor sizes, this will allow our system to operate at variable speed.

The use of asynchronous wound-rotor machines minimizes these factors because most of the power is feeding the grid by the stator and 25% of the total power goes through the rotor with the power converters [1]. This presents an economic advantage as we will minimize losses and cost of production [2].

Another advantage of DFIG is the optimization of wind energy conversion. In order to optimize the wind energy, the wind turbine must be controlled in such a way that the rotor speed adapts to the wind speed so that the specific speed is optimum.

In addition, wind turbines based on DFIG controls the reactive power exchanges with the grid, which avoid the consumption of reactive from such type of generators.

Control of our machine was done by four methods, the first using a PI controller, the second controller with a RST controller and the last one an RST fuzzy logic with virtual reference (VFLC-RST) controls.

This paper is organized as follows; the description of the wind system is presented in section 2. In section 3, the mathematical model and control of DFIG are given. The section 4 focuses on the robust control of the DFIG based an adaptive and virtual fuzzy controller (AFLC-PI and VFLC-RST).

Description of the wind system

The wind system studied in this paper is a three-blade model, it is based on an asynchronous machine double DFIG supply delivering a power of 1.5 MW. The turbine via a gearbox drives the generator, which is connected to the mains by the stator, and also through the three-phase static converter IGBT by the rotor. The latter is provided with rings / brushes systems. The converters machine side network, denoted C- M and C-N respectively are controlled by Width Modulation Pulse (PWM) [1-2-3] (Fig. 1).

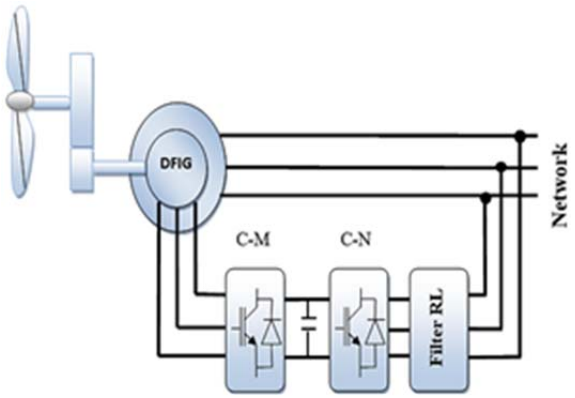

Fig.1. Variable-speed wind system based on DFIG [1-2-3]

Table 1. Parameters for the Wind Power [4]

Components	Part name	Rating values
R	Radius of the wind turbine	35.25 m
G	Gain of the speed multiplier	90
R_s	Statator resistance	0.012 Ω
R_r	Rotor Resistance	0.021 Ω
l_{0s}	Stator leakage inductance	2.0372 e-004 H
l_{0r}	Rotor leakage inductance	1.7507e-004 H
M	Mutual inductance	0.0135 H
j	Inertia of the tree	1000 kg m^2
f	friction coefficient of the DFIG	0.0024
p	Number of pole pairs	2

Modelling and control of DFIG

A. Model of DFIG

To model the induction motor with rotor coil (DFIG), we will rely on simplifying assumptions most commonly seen. We will have the model of DFIG below [6-7] (Fig. 2).

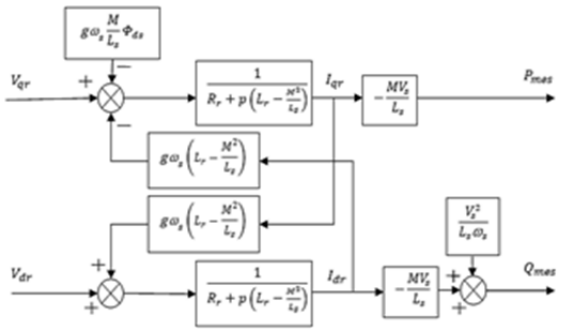

Fig.2. Model of DFIG in the dq plane [1-6-7]

where: $V_{d\text{-}ref}$ et $V_{q\text{-}resf}$: the tensions in the dq rotor reference; i_{dr} et i_{qr} : the rotor currents in the dq reference; Φ_{ds} : the stator flux in the benchmark dq; R_s et R_r : the resistance of stat; or and rotor windings; L_s et L_r :the respective stator and rotor inductances; M : the stator mutual inductance rotor; V_s : Stator voltage; g : Sliding; ω_s : the electrical pulse of the stator currents.; s : Laplace coefficient; $Pmes$: the measured active power; $Qmes$: the measured reactive power.

B. Vector control 0DFIG in generator

The general principle of vector control active and reactive power is shown in the following (fig. 3). [1-6-7].

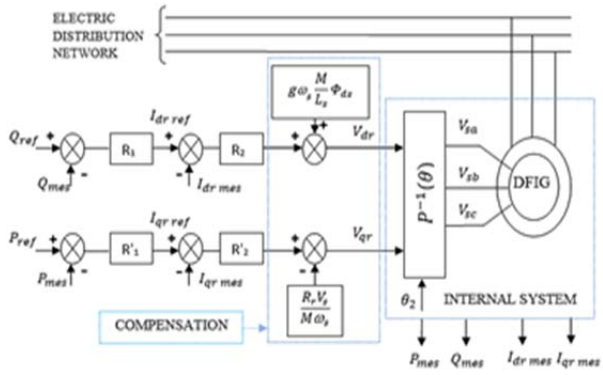

Fig.3. Vector control of DIFG

where: I_{drmes},I_{qrmes} : currents of d and q axis rotor respectively; I_{dref} , I_{qref}: reference current d-axis and q-axis respectively; P_{ref} ,Q_{ref}: Active and reactive power respectively; θ_2 : transformation angle; $P^{-1}(\theta)$: The transformation of PARC.

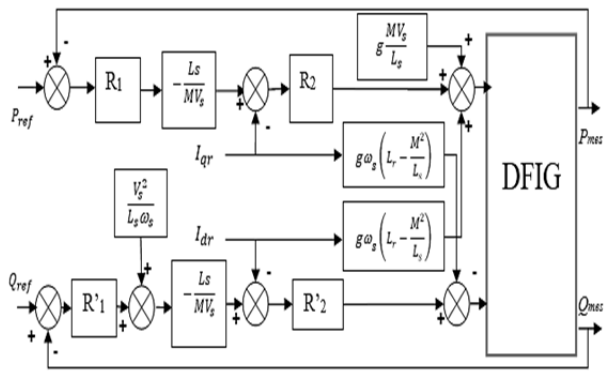

Fig. 4. Indirect control with power loop [1-6-7-8].

Two controllers are present on each axis, R1 and R2 for the d axis, and R'1 and R'2 for the q axis (Fig 4) [1-6-7-8].

C. Performance Analysis

This analysis will be conducted by a simulation using MATLAB-Simulink software. Several tests of performance and robustness will be established to study the viability and robustness of controllers used.

Interpretation of results will be conducted to determine the most appropriate configuration for use in the wind energy sector.

1 Follow-up of instructions:

This test consists of performing active and reactive power steps while maintaining a constant DFIG driving speed under the following test conditions:

Where:

Machine driven at 1400 rev / min.

At t = 1 s: an active power step (Pref) goes from 1MW to -1MW

at t = 2 s: reactive power levels (Qref) Forgot -1 Mvar to 1 Mvar

V_{dc} =200V (DC bus voltage)

f_p =2000 Hz (DC bus frequency).

2 Robustness:

This test consists in varying the parameters of the model of the machine and to see if the regulation remains within the constraints fixed by the specification. Each parameter of the machine will be varied independently of the others. This will allow us to target the quantity for which the previous regulators will not be robust.

To make an objective analysis of the robustness of the control, it is imperative to put it in the most unfavourable conditions allowed by the manufacturer. For this purpose the resistances increase by 50% and the inductances decrease by 50% due to the respective effects of heat and saturation. The speed will be constant 1400 rev / min and f_p = 2000 Hz.

3 Performance:

This test allows us to check to what extent the powers follow their instructions when the speed of rotation of the machine varies abruptly.

We will conduct the test under the following conditions:

At t = 1.5 sec: speed level (Ω) pass 1400 rev / min to 1600 rev / min.

The active power equal to 1 MW.

The reactive power is equal to -1 Mvar.

Study of different methods of control

In the next section, we will check our system with different regulators. For this, we will use for each case of PI, PI-FUZZY, RST, RST-FUZZY at the location provided (R_1, $R_1^{'}$, R_2 & R2') in our model (Fig 4).

A . Vector control of DFIG with PI regulator

1) Principle of the studied regulator

The system is completed is corrected by a PI controller whose transfer function is of the form:

(1) $$K_p + \frac{K_i}{S}$$

They corresponding to the four regulators used in our system [1].

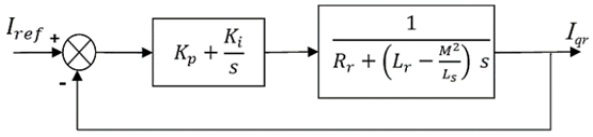

Fig. 5. PI regulator synthesis used in the current loop

were: K_p, K_i : Respectively the proportional and integral gains of the PI controller; I_{ref} : Reference current; I_{qr} : Rotor current measured.

The same is done for the external power loop, and we will have the following results.

2) Simulation results and interpretation

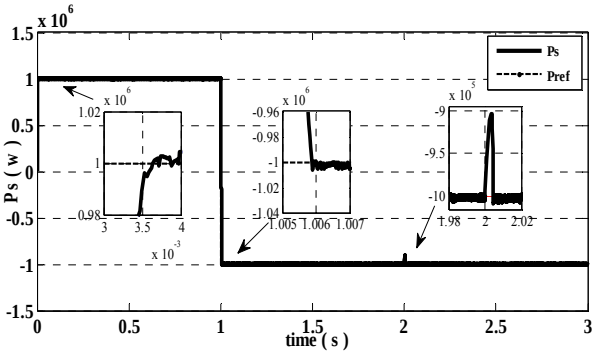

Fig.6. Stator active power (followed set tracking)

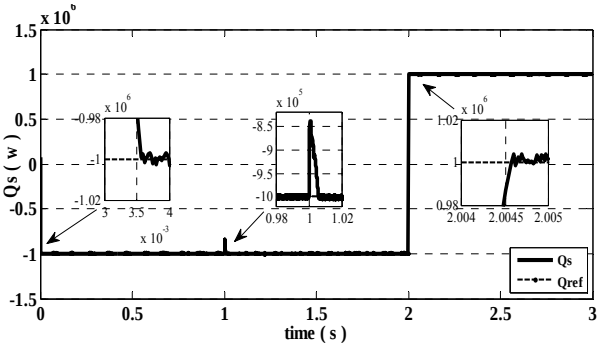

Fig.7. Stator reactive power (followed set tracking)

The followed set is tracked with a delay of 3.65 ms. In the case of a variation in the step from P to t = 1 s, the reported delay is t = 5.58 ms for the active power (Fig 6). And when the reactive power varies at t = 2 s, the reported delay is 4.6 ms (Fig 7).

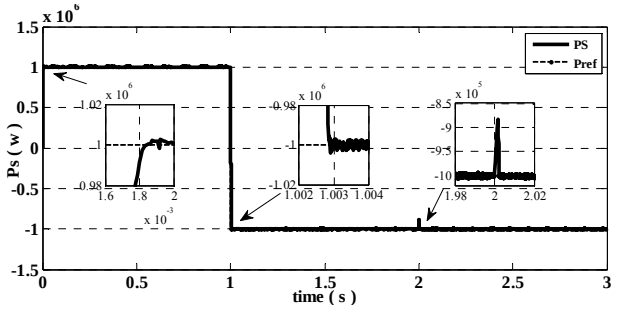

Fig.8. stator active power (variation of inductances)

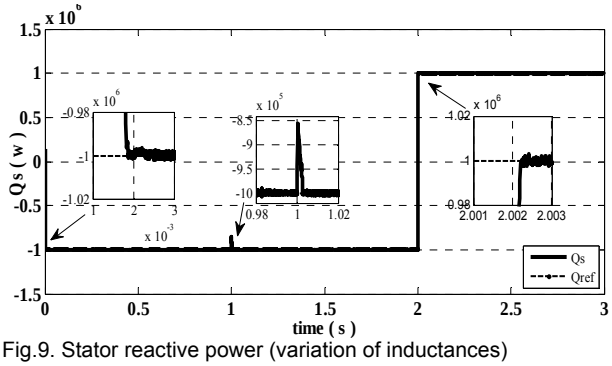

Fig.9. Stator reactive power (variation of inductances)

As far as the decoupling between the direct and quadrature axes is concerned, it should be noted that this is shown in the graph of the reactive power at t = 1s, where there is a disturbance which is 16 % (Fig 7), and Appear in active power at t = 2s worth 9 % (Fig 6)

When the change in inductance of 50 % (Fig 8, 9), we found that in the time to think back a helpless 1.8 ms While variation in the level of P at t = 1s, the reported delay is t = 2.9 ms for the active power (Fig 8). And when reactive power changes at t = 2 s, the reported delay is 2.2ms (Fig 9).

Also it is found that the level of P is accompanied by disruption in the monitoring of the set reactive power or it attaint to 15 % (Fig 9). While the influence of the level of the Q set-point tracking Active Power has also conversed disruption of 12 % (Fig 8).

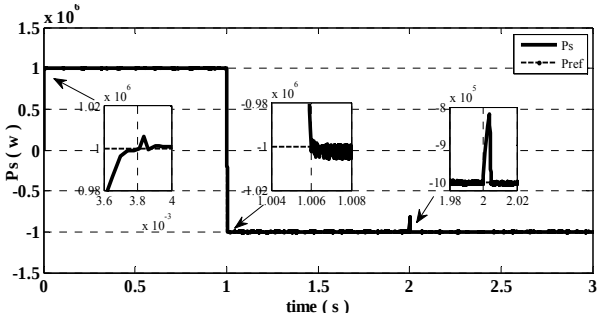

Fig.10. Stator active power (resistance variation)

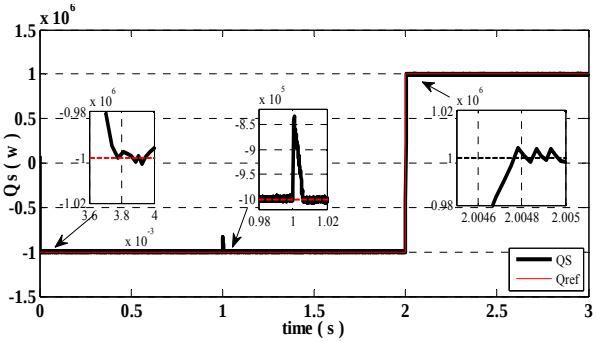

Fig.11. Stator reactive power (resistance variation)

When the resistors have varied from 50% (Fig 10, 11), it was found that the time to look back to increase to 3.75 ms, while when varying the P level at t = 1 s, the reported delay of t = 6 ms for the active power (Fig 10). And when the reactive power varies at t = 2 s, the reported delay is 4.8 ms (Fig 11).

While the disturbance appeared on the monitoring of the set reactive power is 17 % (Fig 11) and that appeared follow the set of active power is 18 % (Fig 10).

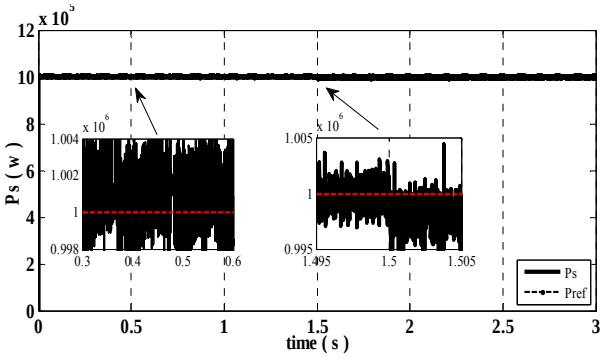

Fig.12. Stator active power (chattering & speed variation)

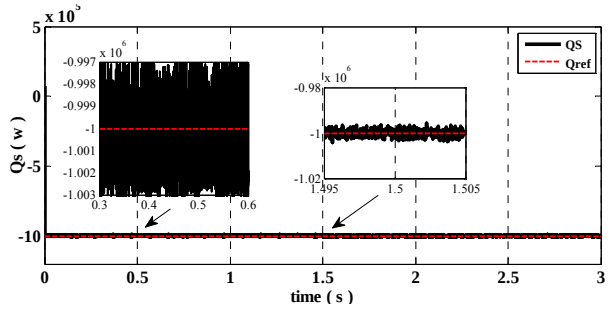

Fig.13. Stator reactive power (chattering & speed variation)

When variation in the speed of wind turbine at t = 1.5 s, it causes a static error in the active power reference tracking (Fig 12). By against, it does not reach that influence the set followed the reactive power (Fig 13).

The effect of chattering see in this control mode varies in a range of ±0.3 % (Fig 12, 13).

B. Vector control of DFIG with FUZZY PI-regulator (PIFLC)

1) Principal of the studied regulator

PI-fuzzy hybrid controllers can be considered as non-linear PI because their parameters change during operation. This approach, which combines the PI controller and the supervisor with fuzzy rules, offers the possibility of using the simplicity of PI controllers and adaptability, the flexibility of the fuzzy controller.

We propose a supervisor whose inputs are the error and its variation, and the outputs are two fuzzy matrices to generate the signals to be applied to each gain of the PI (Fig 14) [9-10].

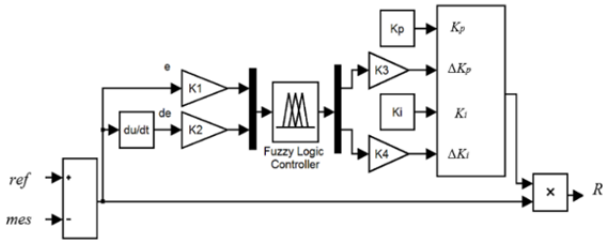

Fig. 14. Structure of adaptive FUZZY PI-regulator

where: *ref* :The reference value (power or current); *mes*: The measured value (power or current); K_1, K_2, K_3, K_4 : The normalization gains (power loop or current loop) ; *Kp, Ki* : The real gains of the PI regulator (power loop or current loop); Kp', Ki': New gains calculated FUZZY PI-controller (power loop or current loop); ΔKp , ΔKi: The normalized values calculated by the regulator FUZZY - (loop power or current loop); *R* : the output of the adaptive controller PI-FUZZY; *e* : The calculated error; *de* :The variation of the error.

The blur system is used to modify the parameters according to the behaviour of the process. In our case, the order gains will be adjusted in real time. They are calculated by equation:

$$(2) \qquad \begin{cases} K_p' = K_p + \Delta K_p \\ K_i' = K_i + \Delta K_i \end{cases}$$

On the other hand, all the rules of fuzzy inference are summarized in the table below [Table 2 and 3].

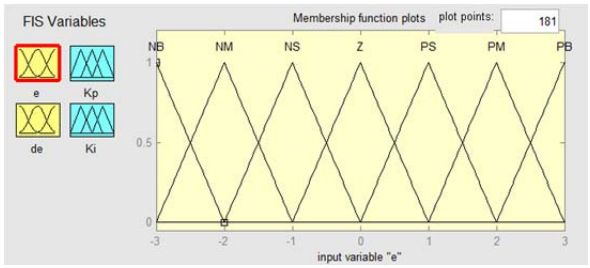

Fig. 15. Membership functions of p and universe of speech (The error« e »)

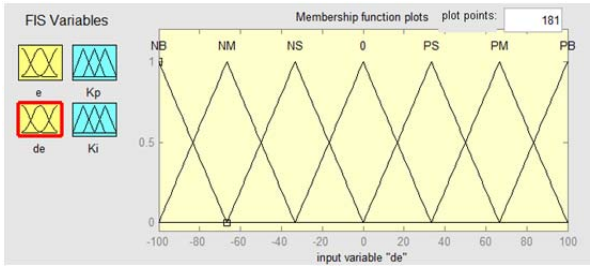

Fig. 16. Membership functions and universe of speech (Variation of the error "de")

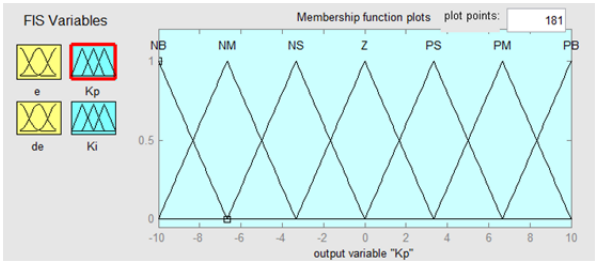

Fig. 17. Membership functions and universe of speech (The calculated normalized values«ΔKp »)

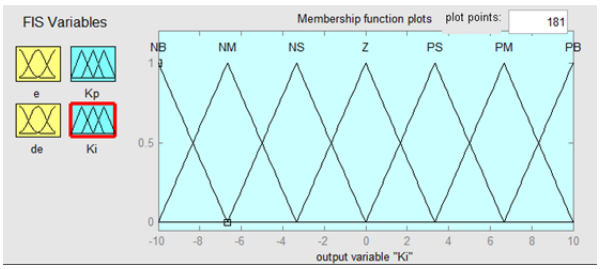

Fig. 18. Membership functions and universe of speech (The calculated normalized values «ΔKi »)

Table 2. Rules for the fuzzy controller (ΔKp) [10]

e	de						
	NB	NM	NS	Z	PS	PM	PB
NB	PB	PB	PM	PM	PS	Z	Z
NM	PB	PB	PM	PS	PS	Z	NS
NS	PM	PM	PM	PS	Z	NS	NS
Z	PM	PM	PS	Z	NS	NM	NM
PS	PS	PS	Z	NS	SS	NM	NM
PM	PS	Z	NS	NM	NM	NM	NB
PB	Z	Z	NM	NM	NM	NB	NB

Table 3. Rules for the fuzzy controller (ΔK i) [10]

e	de						
	NB	NM	NS	Z	PS	PM	PB
NB	NB	NB	NM	NM	NS	Z	Z
NM	NB	NB	NM	NS	NS	Z	Z
NS	NB	PM	NS	NS	Z	PS	PS
Z	NM	NM	NS	Z	PS	PM	PM
PS	NM	NM	Z	PS	PS	PM	PB
PM	Z	Z	PS	PS	PM	PB	PB
PB	Z	Z	PS	PM	PM	PB	PB

2) Simulation results and interpretation

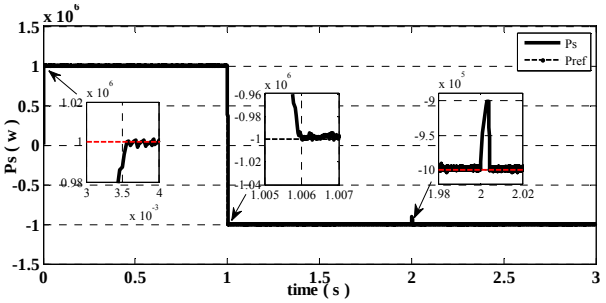

Fig. 19. Stator active power (followed set tracking)

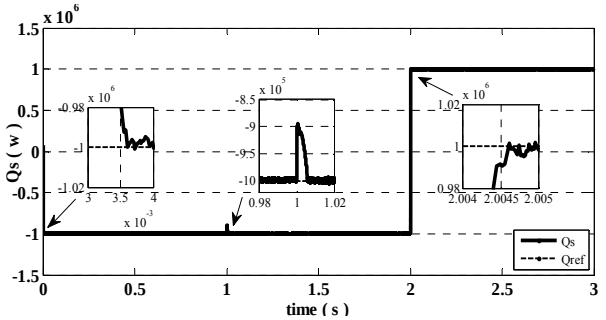

Fig. 20. Stator reactive power (followed set tracking)

The followed set is tracked with a delay of 3.6 ms. While when varying the level of P t =1 s, the reported delay is t=6 ms for the active power (Fig 19). In addition, when the reactive power varies at t =2s, the reported delay is 4.6 ms (Fig 20).

As far as the decoupling between the direct and quadrature axes is concerned, it should be noted that the latter appears in the graph of the reactive power at t = 1 s, where there is a perturbation of 16 % (Fig 20) and Appear in active power at t =2 s where the reported value is 9 % (Fig 19).

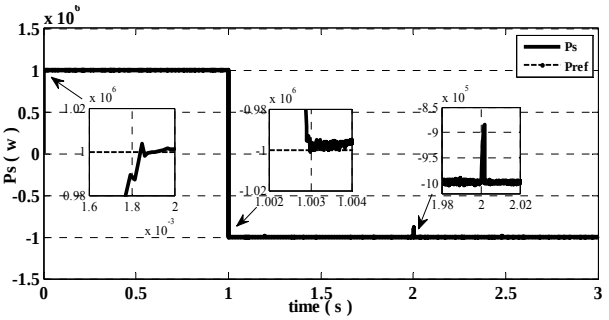

Fig. 21. Stator active power (variation of inductances)

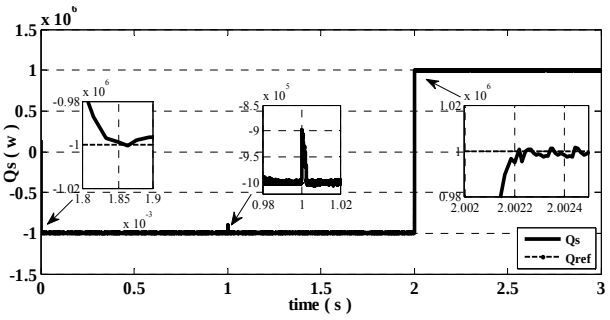

Fig. 22. stator reactive power (variation of inductances)

When the change in inductance of 50% (Fig 21), time to think back to a destitute 1.85 ms While variation in the level of P at t =1 s, the delay is reported T =2.9 ms for the active power (Fig 21). And when the reactive power varies at t =2s, the reported delay is 2.2 ms (Fig 22).

The level of P is accompanied by disruption in the monitoring of the set reactive power or it attaint to 10% (Fig 22). While the influence of the level of the Q set-point tracking active power chatted a disruption of 12% (Fig 21).

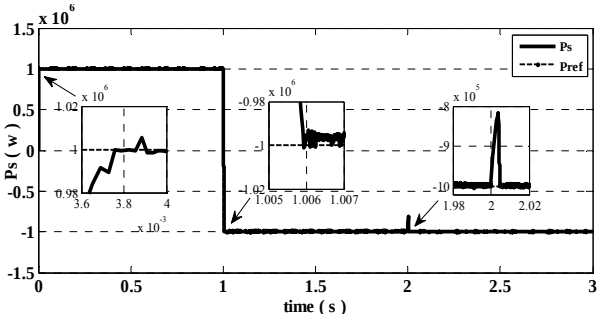

Fig. 23. Stator active power (resistance variation)

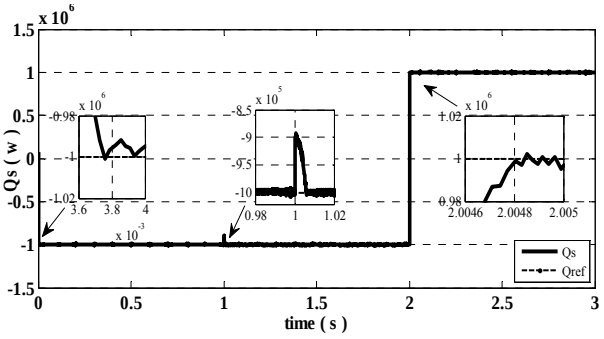

Fig. 24. Stator reactive power (resistance variation)

When the resistors have varied from 50% (Fig 23, 24), it was found that the time to look back to increase to 3.75 ms, while when varying the P level at t =1 s, the reported delay of t = 5.9 ms for the active power (Fig 23). And when the reactive power varies at t =2 s, the reported delay is 4.8 ms (Fig 24).

While the disturbance appeared on the monitoring of the set reactive power is 12 % (Fig 24) and that appeared follow the set of active power is 18 % (Fig 23).

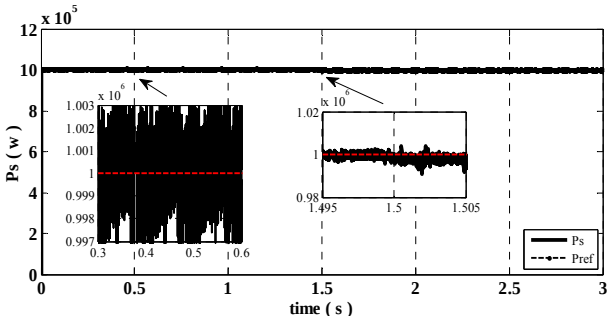

Fig. 25. Stator active power (chattering &speed variation)

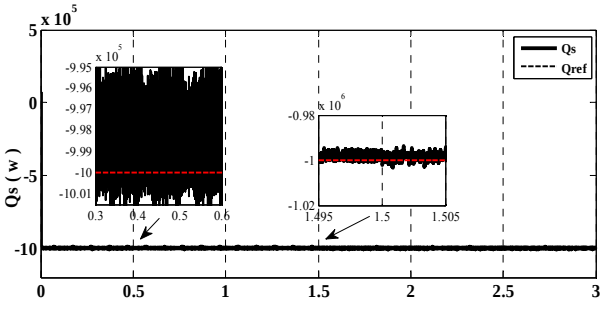

Fig. 26. Stator reactive power (chattering &speed variation)

When variation of wind speed at t = 1.5 s (Fig 25, 26), we see that it has no effect on the set followed with this type of regulator (Fig 25, 26).

The effect of chattering see in this control mode varies in a range of ±0.3% (Fig 25, 26).

C. Vector control of DFIG with an RST controller

1) Principle of the studied regulator

The general form of the regulator RST is that of the figure below (Fig 27) [11].

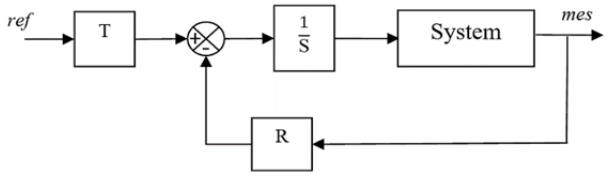

Fig.27. General Form of the RST regulator

In this article, and for power better adapted the RST controller with what the FUZZY examined following, we adopted the shape of the particular case where R = T (Figure 28) [11].

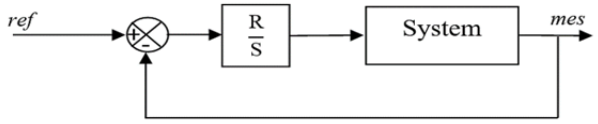

Fig. 28. Form of the particular case of the RST controller

For the internal loop (loop of rotor current) donating regulator are R2 & R'2 (Fig 4), and the transfer function is of first degree, the parameters of the regulator that have been taken are given by the following equation (3).

$$\begin{cases} R = R_1 s + R_0 \\ S = S_1 s + S_0 s \end{cases} \quad (3)$$

where: R_1 , R_0 , S_1 , S_0 : The parameters of the regulator RST of the internal current loop.

For cons, the power loop gift the controller are R1& R'1 (Fig 4), the parameters of the regulator that have been taken are given by the equation (4).

$$\begin{cases} R = R_{2x} s^2 + R_{1X} s + R_{0x} \\ S = S_{2x} s^2 + S_{1x} s + S_{0x} s \end{cases} \quad (4)$$

where: R_{2x} , R_{1X} , R_{0x} , S_{2x} , S_{Ix} , S_{0x}: The parameters of the RST regulator of the external power loop.

2) Simulation results and interpretation

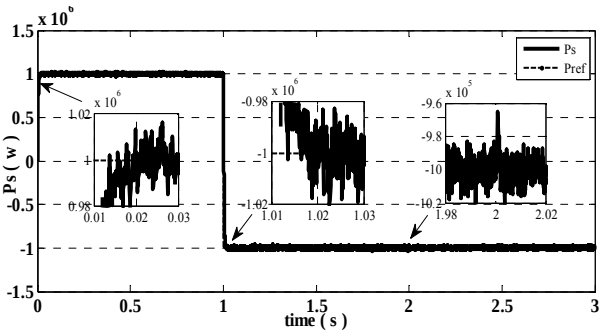

Fig. 29. Stator active power (followed set tracking)

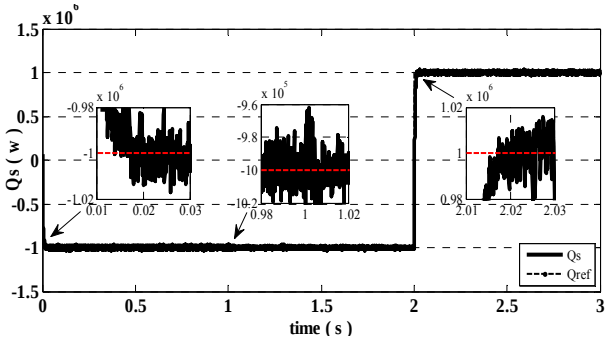

Fig. 30. Stator reactive power (followed set tracking)

The followed set is tracked with a delay of up to 18 ms. While when varying the level of P at t=1 s, the reported delay is t=18 ms for the active power (Fig 29). And when the reactive power varies at t=2 s, the reported delay is 18 ms (Fig 30).

For decoupling between the direct and quadrature axes, it should be noted that the latter appears in the graph of the reactive power at t = 1 s, where there is a disturbance which has reached 5 % (Fig 30) Appeared in the active power at t =2 s with the same value of 5 % (Fig 29).

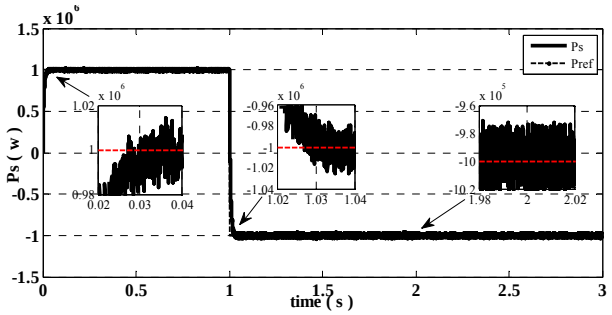

Fig. 31. Stator active power (variation of inductances)

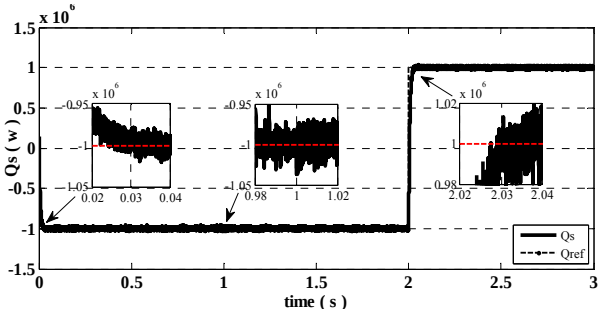

Fig. 32. stator reactive power (variation of inductances)

The change in inductance of 50% (Fig 31, 32) has its influence on the time to think about it, where it increased to 30 ms While variation in the level of P at t=1 s the reported delay is t=30 ms for the active power (Figure 31). And when the reactive power varies at t=2 s, the reported delay is 30 ms (Fig 32).

For decoupling between the direct and quadrature axes, it should be noted that the latter does not appear in the graph of the reactive power (Fig 31), and no longer on the active power (Fig 32).

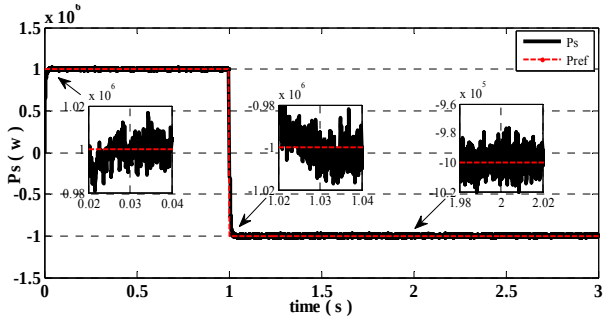

Fig. 33. Stator active power (resistance variation)

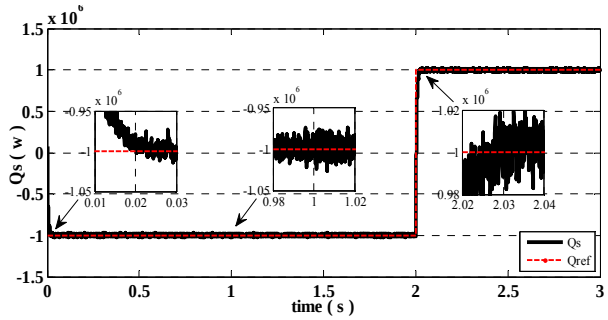

Fig. 34. Stator reactive power (resistance variation)

The variation of the resistances by 50% (Fig 33, 34) also has an influence on the reflection time, when it has decreased to 25 ms, whereas when the step change from P to t = 1 s, the reported delay is also t=25 ms for the active power (Fig 33). And when the reactive power varies at t=2 s, the reported delay is 25 ms (Fig 34).

The step of P has no effect on the reactive power set point follow-up, and the step of Q still has no effect on the set point follow-up of P (Fig 33, 34)

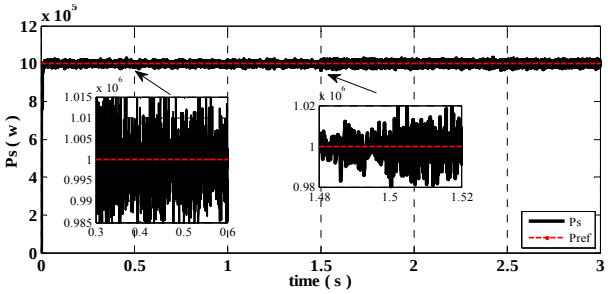

Fig. 35. Stator active power (chattering &speed variation)

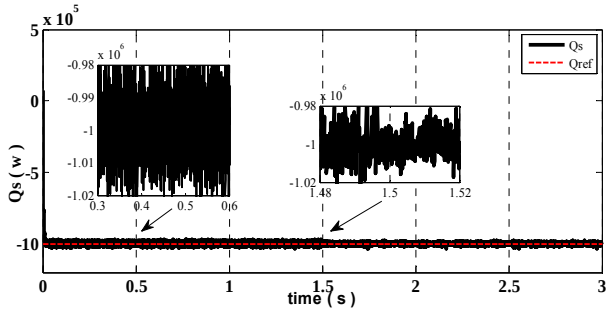

Fig. 36. Stator reactive power (chattering &speed variation)

When the wind speed varies, we see that it does not reach that influence the target followed with this type of regulator (Fig 35 and 36).

The chattering effect observed in this mode of control varies within a range of 1.5% for active power and 2% for the reactive power (Fig 35 and 36).

D. Vector control DFIG with a RST-FUZZY-controller virtual reference

1) Principle of the studied regulator

In this type of control we will proceed with both techniques at once, the first and that of the RST-FUZZY control virtual reference applied in the power loop (Fig 37), and the second and the composite RST-FUZZY applied in the inter loop current (Fig 41) [9].

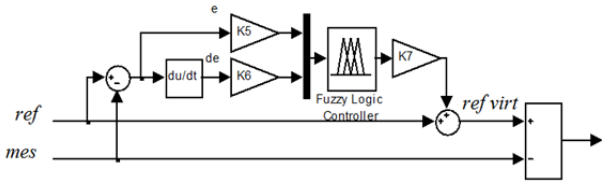

Fig. 37. Structure Fuzzy virtual reference regulator

where: ref_{virt}: The virtual reference value (power or current); K_5, K_6, K_7: Standardization gains (power loop).

For this control mode the membership functions for the input and output variables respectively, and their speech universes, are chosen (Figure 38, 39 and 40). On the other hand, all the rules of fuzzy inference are summarized in the table below [Table 4].

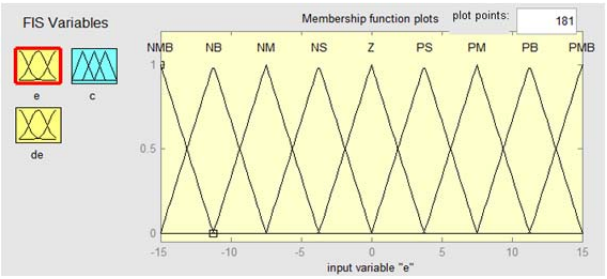

Fig. 38. Membership functions and universe of speech (The error « de »)

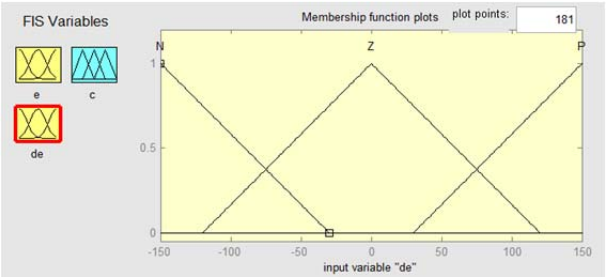

Fig. 39. Membership functions and universe of speech (Variation of error« de »)

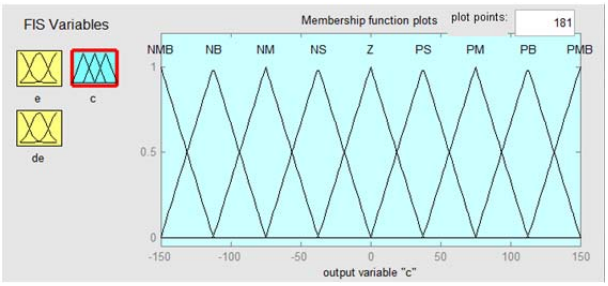

Fig. 40. Membership functions and universe of speech (The normalized values calculated by the controller)

Table 4. Rules for the fuzzy controller (power loop)

de	e								
	NMB	NB	NM	NS	Z	PS	PM	PB	PMB
N	NMB	NB	NM	NS	NS	Z	PS	PM	PB
Z	NMB	NB	NM	NS	Z	PS	PM	PB	PMB
P	NB	NM	PS	Z	PS	PS	PM	PB	PMB

For the current loop, a simpler and simpler method was used which gave us good results at the response time (Figure 41), but this is due to overshoot because of the speed of the regulator RST of the internal loop (R2 and R'2) which and of the first degree

For this control mode the membership functions for the input and output variables respectively, and their speech universes, are chosen (Figure 38, 39 and 40). On the other hand, all the rules of fuzzy inference are summarized in the table below [Table 4].

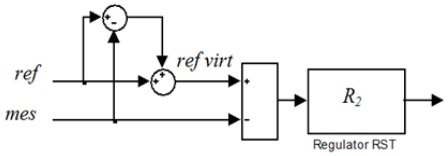

Fig. 41. Structure of the Virtual Reference current loop

Subsequently, a fuzzy regulator is added to the previous structure which makes it possible to improve directly the behavior, in order to attenuate the overrun by superimposing itself on the existing control. Technique called composite command (Fig 42) [9-12-13].

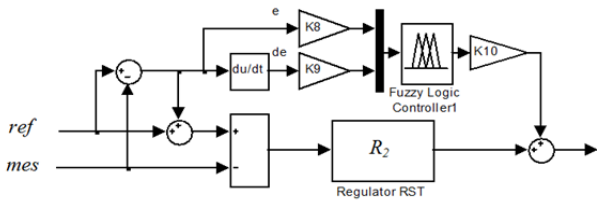

Fig. 42. RST-composite FUZZY control

where: K_8, K_9, K_{10}: The normalization gains (internal current loop).

In this regulator, the membership functions of the input variables and output respectively, and their universe of discourse, appear in the figures (Fig 43, 44, 45). On the other hand, all the rules of fuzzy inference are summarized in the table below [Table 5].

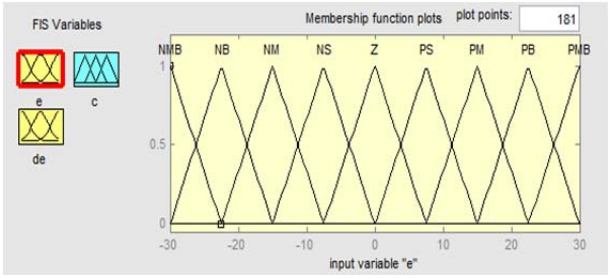

Fig. 43. Membership functions and universe of speech (The error« de »)

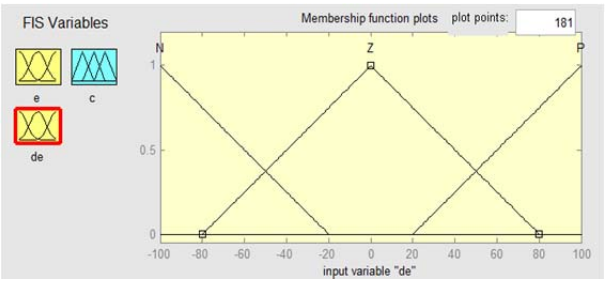

Fig. 44. Membership functions and universe of speech (Variation of error« de »)

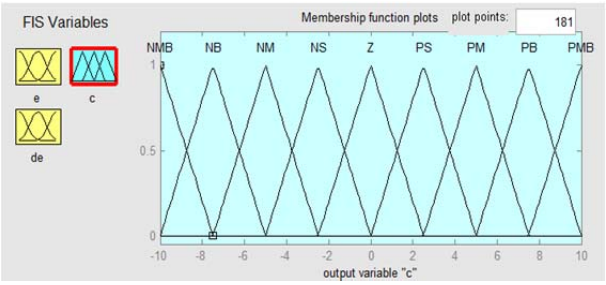

Fig. 45 Membership functions and universe of speech (The normalized values calculated by the controller)

Table 5. Rules for the fuzzy controller (current loop)

de	e								
	NMB	NB	NM	NS	Z	PS	PM	PB	PMB
N	NMB	NB	NM	NS	NS	Z	PS	PM	PB
Z	NMB	NB	NM	NS	Z	PS	PM	PB	PMB
P	NB	NM	PS	Z	PS	PS	PM	PB	PMB

2) Simulation results and interpretation

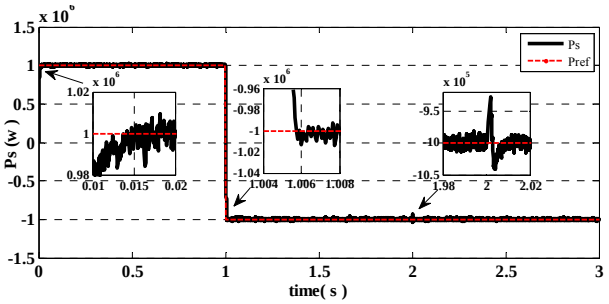

Fig. 46. Stator active power (set point tracking)

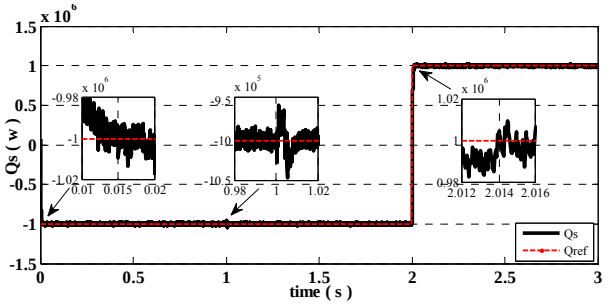

Fig. 47. Stator reactive power (set point tracking)

The followed set is tracked with a delay of up to 14 ms. While when varying the level of P at t=1 s, the reported delay is t=5.8 ms for the active power (Fig 46). And when the reactive power varies at t=2s, the reported delay is 14 ms (Fig 47).

As far as the decoupling between the direct and quadrature axes is concerned, it should be noted that the latter appears in the graph of the reactive power at t=1 s, where a disturbance is observed which has reached 4%

(Fig 47), and appears in the active power at t=2 s of a value of 7 % (Fig 46).

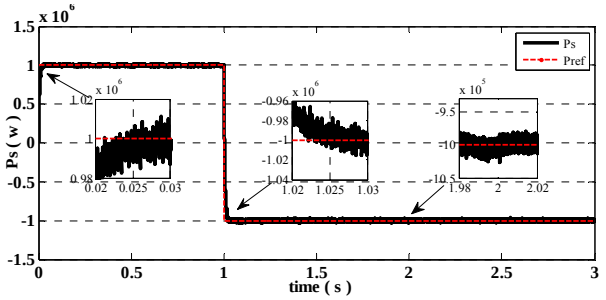

Fig. 48. Stator active power (variation of inductances)

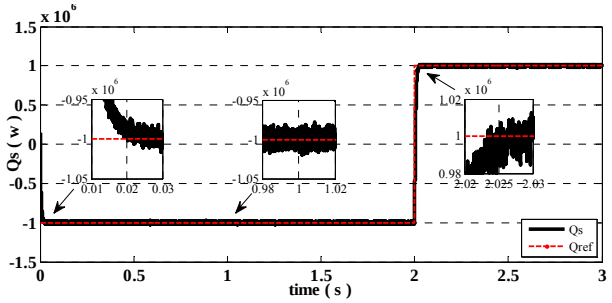

Fig. 49. Stator reactive power (variation of inductances)

The variation of the inductance of 50 % (Fig 48, 49) has an influence on the reflection time, where it has reached a value of 24 ms, as well as on variation of the step from P to t=1 s, the reported delay of t=24 ms for the active power (Figure 48). And when the reactive power varies at t=2s, the reported delay is 25 ms (Fig 49).

For the decoupling between the direct and quadrature axes, it should be noted that the latter does not appear in the graph of the reactive power (Fig 48), and no longer on the active power (Fig 49).

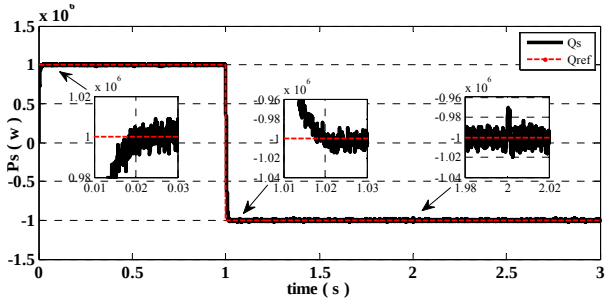

Fig. 50. Stator active power (resistance variation)

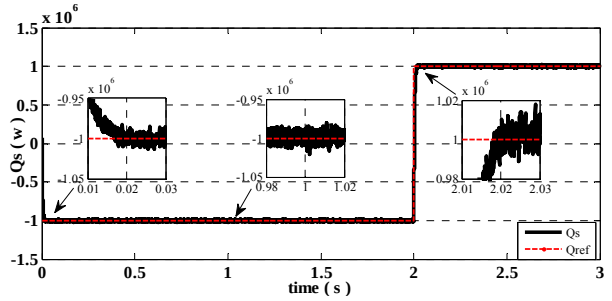

Fig. 51. Stator reactive power (resistance variation)

If the resistance varies by 50 % (Fig 50, 51), the time to look back increases to 18 ms, while when varying the level of P at t=1 s, the delay is reported t=20 ms for the active power (Fig 50). And when the reactive power varies at t=2 s, the reported delay is 18 ms (Fig 51).

While the disturbance appeared on monitoring the set of active power is 4 % (Fig 50), while the resistance change has no impact on the reactive power (Fig 51).

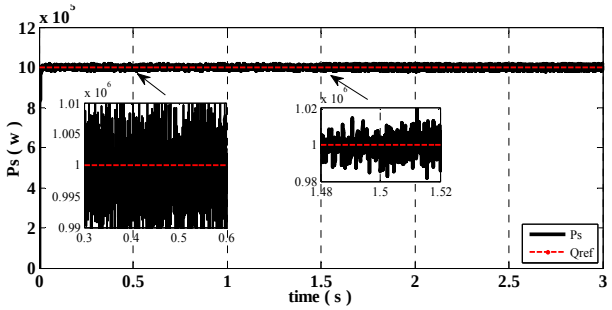

Fig. 52. Stator active power (chattering &speed variation)

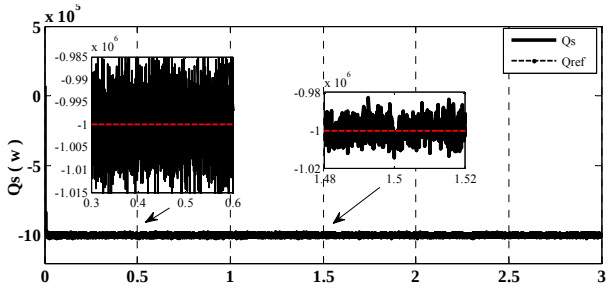

Fig. 53. Stator reactive power (chattering & speed variation)

When the wind speed varies suddenly, we see that it has no influence on the set followed with this control mode (Fig 52 and 53).

The chattering effect observed in this mode of control varies within a range of ±1% for active power and 1.5% for the reactive power (Fig 52 and 53).

Comparison of results

The four control strategies studied above compared in this part, where we will analyze the different results obtained by simulation [Table 6, 7, 8].

Table 6. Comparisons for the control strategies

Control	Response time (ms)			Decoupling%		Chattering%	
	t=0s	t=1s	t=2 s	P	Q	P	Q
PI	3.65	5.58	4.6	9	16	±0.3	±0.3
AFLC-PI	3.6	6	6.6	9	16	±0.3	±0.3
RST	18	18	18	5	5	±1.5	±2
VFLC-RST	14	5.8	14	7	4	±1	±1.5

Table 7.Comparisons for the control strategies (L -50%)

Control	Response time (ms)			Decoupling %	
	t=0 s	t=1 s	t=2 s	P	Q
PI	1.8	2.9	2.2	12	15
AFLC-PI	1.85	2.9	2.2	12	10
RST	30	30	30	/	/
VFLC-RST	24	24	25	/	/

Table 8.Comparisons for the control strategies (R +50%)

Control	Response time (ms)			Decoupling %	
	t=0 s	t=1 s	t=2 s	P	Q
PI	3.75	6	4.8	18	17
AFLC-PI	3.75	5.9	4.8	18	12
RST	25	25	25	/	/
VFLC-RST	18	20	18	4	/

For the PI control and AFLC-PI control, and From the perspective of think back of the times, we see that the control AFLC-PI regulator to give the same results as the PI

control, but when variation of internal parameters and / or the change in speed, the AFLC-PI give more stability and robustness.

For this purpose the AFLC-PI controller is more robust than the PI controller.

For the RST control and the VFLC-RST control, it is noted that the VFLC-RST control is more dynamic and robust than that of the RST control, from all points of view.

But if we compare AFLC-PI and VFLC-RST, the AFLC-PI control is more dynamic, but the VFLC-RST is more robust.

Conclusion

In this paper, an adaptive fuzzy controller (AFLC-PI and VFLC-RST) have been evaluated for a DFIG for Improvement of power flow performance.

The simulation results show that improved performance has been achieved by these controllers as compared to PI and RST controls. PI and RST control can cause large interactions between the current loops when the transmission system parameters are actually known

An AFLC-PI and VFLC-RST controller produces better transient response and improved robustness with respect parameters fluctuations such as the transmission line parameter which is allowed to vary within a large range without significantly influencing their performance.

***Authors**: Abdelkader Abdallah Laboratory SCAMRE Department of Electrical Engineering, E.N.P Oran BP 1742 El' M'naouer, Oran, Algeria, Email: abdallah_aek@yahoo.fr; Abdelkader Chaker, Laboratory SCAMRE Department of Electrical Engineering, E.N.P Oran BP 1742 El' M'naouer, Oran, Algeria, Email: chakeraa@yahoo.fr; Tayeb Allaoui, Laboratory L2GEGI, University Tiaret BP 78 Zaaroura, Tiaret, Algeria.*
Email: allaoui_tb@yahoo.fr.

REFERENCES

[1] A. Abdallah, A. Chaker, and T. Alaoui, "Contrôle d'un aérogénérateur pour la production d'énergie électrique, [Deuxième Conférence Internationale Sur La Maintenance, La Gestion, La Logistique Et L'électrotechnique, Enset Oran, Algérie, 2012].

[2] A. Mirecki, Etude comparative de chaînes de conversion d'énergie dédiées à une éolienne de petite puissance, Thèse de doctorat de l'institut national polytechnique, Toulouse, 2005.

[3] A. Gaillard, Système éolien basé sur une MADA contribution à l'étude de la qualité électrique et la continuité de service, Thèse de doctorat, Université Henri Poincaré, Nancy-I, 2010.

[4] S. El Aimani, Modélisation de différentes technologies éoliennes intégrées dans un réseau de moyenne tension, thèse de doctorat de l'Ecole Centrale de Lille et l'Université des Sciences et Technologies de Lille, France, 2004.

[5] B. Multon, Equipe SETE, Aérogénérateurs électriques, Master Recherche STS IST-SPEE Paris 11, Ecole Normale Supérieure de Cachan - SATIE UMR CNRS-ENS Cachan 8029, Antenne de Bretagne, 2009.

[6] F. Poitiers, Etude et commande de génératrices asynchrones pour l'utilisation de l'énergie éolienne, Thèse de doctorat, Ecole polytechnique de l'université de Nantes. 2003.

[7] R. Abdessemed, "Modélisation Et Simulation Des Machine Electrique", Ellipses, Paris, 2011.

[8] A. Boyette, Contrôle-commande d'un générateur asynchrone à double alimentation avec système de stockage pour la production éolienne, Thèse de doctorat, Université Henri Poincaré, Nancy-I, 2006.

[9] P. Borne, J. Rozinoer, J Yves. Dieulot, L. Dubois, Introduction à la Commande Floue, Editions Technip, Paris, 1978.

[10] E P. Dadios (2015), Fuzzy Logic - Tool for Getting Accurate Solutions, ISBN 978-953-51-2153-4, INTECH, 49-77).
https://www.intechopen.com/books/fuzzy-logic-tool-for-getting-accurate-solutions/application-of-fuzzy-logic-control-for-grid-connected-wind-energy-conversion-system

[11] D. Lequesne, Réglage P.I.D, Lavoisier, Pris, 2009.

[12] F. Poitiers, T. Bouaouiche, M. Machmoum, Advanced control of a doubly-fed induction generator for wind energy conversion, Electric Power Systems Research, vol. 79, pp.1085–1096, 2009.
http://dx.doi.org/10.1016/j.epsr.2009.01.007

[13] M. Zerikat, S. Chekroun, , A. Mechernene (2010), " Development And Implementation Of High-Performance Variable Structure Tracking For Induction Motor Using Fuzzy-Logic Controller," International Review of Electrical Engineering (IREE), 5 (1), pp. 160-166.